

Scaling and Eigenmode Tests of the Improved Fat Clover Action

Mark Stephenson and Carleton DeTar

Department of Physics, University of Utah, Salt Lake City, UT 84112, USA

Thomas DeGrand and Anna Hasenfratz

Department of Physics, University of Colorado, Boulder, CO 80309, USA

(May 1, 2018)

We test a recently proposed improved lattice-fermion action, the fat link clover action, examining indicators of pathological small-quark-mass lattice artifacts (“exceptional configurations”) on quenched lattices of spacing 0.12 fm and studying scaling properties of the light hadron spectrum for lattice spacing $a = 0.09$ and 0.16 fm. We show that the action apparently has fewer problems with pathological lattice artifacts than the conventional nonperturbatively improved clover action and its spectrum scales just as well.

I. INTRODUCTION

The goal of lattice fermion improvement schemes is to increase the effectiveness of computer algorithms by significantly reducing lattice artifacts at economically coarse lattice spacings, particularly in the range $a < 0.15$ fm. The clover action with the clover coefficient chosen nonperturbatively [1] (NPCA) has been found to give a substantially better scaling of the hadron spectrum over the range [0.06, 0.16] fm than the conventional Wilson fermion action (WA) [2,3]. However, as the lattice spacing is increased over this range, the NPCA becomes increasingly sensitive to local fluctuations in the gauge configurations that produce unwanted artifact singularities at small, positive quark mass, the so-called “exceptional configurations.” To avoid them, one must keep the quark mass artificially high. At increasingly coarse lattice spacing, the lower bound on “safe” quark masses rises, making an extrapolation to physical quark masses increasingly problematical. Difficulties with such “exceptional” configurations are overcome in a variety of approaches, including pole shifting [4] and schemes which implement an exact chiral symmetry on the lattice, the overlap formalism [5], and the domain wall approach [6]. Such methods are computationally expensive. Here, we consider a new (approximate) improvement scheme, the “fat clover” action.

The “fat clover” action (FCA), proposed by DeGrand, Hasenfratz, and Kovács [7], couples the standard clover action to a locally smoothed gauge field. Smoothing of the gauge fields is achieved through a series of APE blocking steps [8]. It is intended that the number of blocking steps remains fixed as the continuum limit is approached. Thus the fermion-gauge coupling is modified at a scale that is a fixed multiple of the cutoff, and the correct local action is recovered in the limit. Smoothing has a number of beneficial effects: lattice artifacts are suppressed, chiral properties are improved, and the renormalization of a variety of lattice quantities, such as the local-vector-current and axial-vector-current renormalization constants Z_V and Z_A , is small [7,9].

Here we examine two variants of fat link actions: one using the tree level value for the strength of the clover term (TFCA) and one using an optimized value (OFCA). (See Table I for a guide to our abbreviations.)

We first study the distribution of real eigenmodes of the lattice Dirac operator in an ensemble of gauge configurations, with particular attention to the “exceptional” eigenvalues at positive quark mass. We show that the FCA has improved chiral properties, in the sense that the spread of leading near zero modes is narrower than with the NPCA at a lattice spacing of 0.12 fm. Thus the “safe” lower bound on quark masses is lower with the FCA. We then present a study of fluctuations in the pion correlator as a qualitative test of the suppression of exceptional configurations in NPCA and TFCA.

Finally we perform a small scaling test of the quenched hadron spectrum for the TFCA and OFCA. Scaling is tested as the lattice constant is varied from 0.092 fm to 0.164 fm, choosing some fixed value of the quark mass, such that either $m_\pi^2 = 2.5\sigma$, where σ is the string tension, or $m_\pi/m_\rho \approx 0.7$ [7]. Included for comparison are the corresponding results for the standard Wilson action (WA), nonperturbative clover action (NPCA), and the standard Wilson action on a fat link background (FWA). In this scaling study we pay careful attention to the elimination of a variety of sources of systematic error: we scale all quantities with physical dimensions and fix the lattice dimensions in physical units.

In Sec. II we give details of the FCA and our computational method. In Sec. III we present results of our lattice simulations. We conclude with Sec. IV.

II. COMPUTATIONAL METHOD

A. Fat Clover Action

The fat clover action (FCA) is the usual clover action

$$S_{SW} = \bar{\psi}M(\kappa)\psi = S_W - \kappa c_{SW} \sum_{\mu < \nu} \bar{\psi}(x)\sigma_{\mu\nu}P_{\mu\nu}\psi(x) \quad (1)$$

where S_W is the Wilson action, and $P_{\mu\nu}$ is the standard ‘‘clover’’ expression for the field strength tensor $F_{\mu\nu}$, except that all link variables in S_W and $P_{\mu\nu}$ are fat links. The fat link is constructed from the original (‘‘thin’’) links with a series of APE blocking steps [8]. A single step creates a new gauge configuration with each gauge link replaced by a weighted sum of the link and its staples, followed by a projection back to SU(3). Explicitly, each link $U_{x,\mu}$ is replaced by

$$V_{x,\mu} = \mathcal{P} \left[(1-c)U_{x,\mu} + \frac{c}{6} \sum_{\nu \neq \mu} \left(U_{x,\nu}U_{x+\nu,\mu}U_{x+\mu,\nu}^\dagger + U_{x-\nu,\nu}^\dagger U_{x-\nu,\mu}U_{x-\nu+\mu,\nu} \right) \right]. \quad (2)$$

where \mathcal{P} represents the projection, which in SU(3) chooses the unique group element U of SU(3) maximizing $\text{Tr}(UV^\dagger)$. (Replacement occurs after all smooth links for the lattice are computed.) This process is repeated $N = 10$ times in our study with a coefficient $c = 0.45$. Such a choice was found to give good stability in instanton size and placement during smoothing in both SU(2) and SU(3) [10,11]. We have not explored other choices extensively, but suspect considerable latitude is permitted in the choice of c and N . After smoothing, the mean plaquette of the fat link is close to 1: For $6/g^2 = 5.7$, the mean plaquette is $\text{Tr}U_{\text{plaq}}/3 = 0.985$ and for $6/g^2 = 6.0$ it is 0.994.

Fat link clover actions, like all clover actions, have no $O(a)$ nor $O(g^2a)$ corrections as long as the clover coefficient c_{SW} is taken to approach unity in the $g \rightarrow 0$ limit. In perturbation theory [12] the effect of the fat link is to multiply the usual thin link quark-gluon vertices by a form factor $(1 - \frac{c}{3}a^2\hat{q}^2)^N$ with $\hat{q}_\mu = (2/a)\sin(q_\mu a/2)$, where q is the gluon momentum. This easily accounts for the observed considerable reduction in additive quark mass renormalization and finite renormalization constants for vector and axial currents close to unity.

The clover coefficient c_{SW} is *a priori* unspecified. We expect, based on the near unit value of the mean plaquette, that an optimal value for simulations would be close to the tree-level value of unity, and that is what one would choose in a tadpole-based improvement program [13]. We chose the value of c_{SW} using the approach of DeGrand, Hasenfratz and Kovačs, based on the position of real eigenmodes of the Dirac operator [7].

To locate the real eigenmodes, for each configuration we calculated a noisy estimator of the expectation value $\langle \bar{\psi}\gamma_5\psi \rangle$ [7,14,15]

$$A(\kappa) = \bar{\eta}\gamma_5 M^{-1}(\kappa)\eta \quad (3)$$

at a closely spaced series of real values κ , where η is an arbitrary random vector, held constant for the scan over κ . A real eigenvalue of $M(\kappa)$ appears as a pole in $A(\kappa)$, provided the corresponding eigenvector has nonzero overlap with the vector η . The quantity $\bar{\eta}M^{-1}(\kappa)\eta$ would also diverge at a real eigenvalue of $M(\kappa)$, but since the real eigenmodes of $M(\kappa)$ are also close to being eigenmodes of γ_5 with eigenvalue ± 1 , the factor γ_5 helps to distinguish them.

In the continuum limit the only real eigenvalues of $M(\kappa)$ are chiral zero modes, occurring at $\kappa_c = 1/8$, i.e. zero bare quark mass. If the lattice Dirac operator is not chiral, the real modes are spread around κ_c (defined as the value of κ where $m_\pi^2(\kappa)$ extrapolates to zero), and can also be shifted from the chiral $\kappa_c = 1/8$ value. Such real eigenmodes are undesirable lattice artifacts that prevent lattice simulations at small quark mass. [16]. Configurations that produce them are called ‘‘exceptional’’, although the problem really lies with the choice of fermion action and not with the gauge configuration itself. Actions with improved chiral properties have real eigenmodes that cluster more closely around κ_c . For such actions it should be possible to study lower quark masses without encountering difficulties with exceptional configurations, or to carry out a simulation on a coarser lattice at the same quark mass.

For a sufficiently high degree of fattening one can optimize the clover coefficient by minimizing the spread of the real eigenmodes on Monte Carlo-generated configurations. In this work, however, we choose a simpler approach. We generate a series of artificial lattice instantons of varying size $a < r_0 < 3a$ on 8^4 lattices and of size $2a < r_0 < 6a$ on 12^4 lattices. Instanton studies at $6/g^2 = 5.7$ and $6/g^2 = 6.0$ predicted instanton sizes in this range [17]. For each such gauge configuration, we examined the position of the resulting fermion real eigenmode. Results are shown in Tables II and III and Fig. 1. For large r_0 the near-zero modes are quite close to zero quark mass. As r_0 drops below the lattice cutoff, the would-be zero mode moves toward negative quark mass. The trajectory of real eigenmodes is altered by

adjusting the clover coefficient c_{SW} . We find that with $c_{SW} = 1.2$ the variation in pole position is minimized for instanton sizes in the range $r_0 > a$. With $c_{SW} = 1.1$ the variation in pole position is minimized for $r_0 > 2a$. Since our scaling test considers lattices over a range of spacings varying by a factor of 2, we choose $c_{SW} = 1.2$ for our coarsest lattice spacing and $c_{SW} = 1.1$ for our finest lattice spacing to assure scaling consistency. We call the action with tuned clover coefficient the “optimized fat clover action” (OFCA). To test sensitivity to this choice, we also present results with the tree-level choice $c_{SW} = 1$ (TFCA).

B. Computational Parameters

There are two parts to this study: an analysis of the distribution of low energy real eigenvalues and an analysis of the scaling of the spectrum. For studies of the distribution of near-zero eigenvalues at $6/g^2 = 5.85$ we analyzed 100 configurations of size 10^4 , and for the companion spectrum study to relate the pion mass to the κ value, 20 configurations of size $12^3 \times 48$. For the spectrum scaling studies we have worked with two ensembles of quenched gauge configurations generated with the conventional one-plaquette Wilson action: 120 configurations of size $8^3 \times 24$ at $6/g^2 = 5.7$ and 100 of size $16^3 \times 48$ at 6.0, corresponding to lattice spacing $a = 0.164$ and 0.092 fm, respectively, based on recent measurements of the string tension for this action in lattice units [18] and the choice $\sqrt{\sigma} = 468$ MeV [19].

The lattice dimensions for the scaling study were chosen to keep an approximately constant physical volume, so as to avoid inconsistent finite size effects. To allow tuning of the quark mass, either by fixing the pion mass in terms of the string tension or in terms of the rho mass, we calculate the spectrum for (typically) three neighboring κ values selected so that the desired dimensionless ratios can be reached by interpolation. Quark propagators were generated from a fixed Gaussian (shell-model) source with standard deviation $2a$ for the coarsest lattice and $4a$ for the finest. Our scaling tests were computed at three values of the clover coefficient c_{SW} for each gauge coupling: $c_{SW} = 1.1$ or 1.2 , as noted above, for the OFCA, $c_{SW} = 1$ for the tree-level fat clover action (TFCA), and $c_{SW} = 0$ for the fat Wilson action (FWA) to test the relative merits of smoothing and reducing the $O(a)$ errors in the action.

III. RESULTS

A. Fermion eigenmodes

For each of the actions in our study we determined the distribution of the real eigenmodes on a set of 100 10^4 gauge configurations, generated with the conventional single plaquette action at $6/g^2 = 5.85$. We determined the probability distribution $P(m_\pi^2)$ of the leading pole (i. e. the eigenvalue corresponding to the largest quark mass) for the various actions in our study.

Note that this statistic is different from the eigenvalue histograms of Ref. [7], where *all* the low energy eigenmodes were included to study the spread of the physical modes. Since here we consider only the pole corresponding to the largest mass on each configuration, these plots are indicative of the exceptional configurations.

To compare leading-pole distributions from the various actions, we converted the κ values to m_π^2 values, by measuring the hadron spectrum with the same action on a set of 20 $12^3 \times 48$ quenched configurations. Results are shown in Fig. 2. Pion masses used for constructing the linear scale conversion, $m_\pi^2 = a/\kappa + b$ are given in Tables IV and V. The bin widths in this figure are variable, since the poles were located by scanning at the same constant increment in κ for all actions. We took this interval as the resolution of the pole location. The corresponding interval in m_π^2 , however, varied from action to action. The bin heights are scaled so that the probability distributions all have unit total area. The TFCA and OFCA actions clearly produce distributions that are more sharply clustered around $m_\pi^2 = 0$. The peak for the OFCA appears at a nonzero bin in m_π^2 , but we estimate a combined systematic and statistical error (one sigma) of one bin width arising from the conversion from κ to m_π^2 near zero pion mass.

To put these results in another perspective, we have also measured the ratio m_π/m_ρ for these configurations. For our sample of gauge configurations at $\beta = 5.85$ the NPCA encounters its first pole at $m_\pi/m_\rho = 0.56(4)$, the TFCA, at about $0.37(6)$ and the OFCA at about $0.42(5)$.

B. Pion Correlators

While a pole in the quark propagator at $\kappa < \kappa_c$ is the most precise indicator of an exceptional configuration, fluctuations in a hadron correlator, e.g. the pion correlator, give a qualitative indication. Poles in the quark propagator

typically have residues with concentrated support in Euclidean space-time. For instanton-induced poles, localization of the residue comes from localization of the zero eigenmode. Since the pion propagator is the gauge-invariant square of the quark propagator, a nearby exceptional pole typically contributes a strong localized fluctuation in the pion correlator—in some cases inducing a “W” shape in a semilog plot.

Starting from a common sample of 80 quenched single-plaquette $8^3 \times 24$ gauge configurations at $6/g^2 = 5.7$, we compute the pion correlator for the NPCA and TFCA for a range of quark masses. We then consider two measures of fluctuations: (1) the noise to signal ratio of the correlator at a fixed time and (2) the number of outliers, based on a correlated chi square measure.

The simplest measure of fluctuations is the noise to signal ratio in a correlator, namely the ratio of the standard deviation of a correlator $\sigma(t)$ to the value of the correlator, $\bar{c}(t)$, as a function of distance and/or quark (or pion) mass. The pseudoscalar correlator is the most useful one to look at, since simple theoretical arguments suggest that $\sigma(t)/\bar{c}(t)$ should be roughly independent of the quark mass. In Fig. 3 this ratio at $t = 10$, namely $\sigma(10)/\bar{c}(10)$, is plotted over a range of m_π/m_ρ for the NPCA and TFCA. It is clear that for $0.5 < m_\pi/m_\rho < 0.7$, fluctuations are dramatically reduced with the TFCA.

We denote the correlator on the i th configuration by $c_i(t)$ and its mean over the sample of configurations by $\bar{c}(t)$. For the outlier test we start by constructing the usual covariance matrix $v_{t,t'}$, based on the observed fluctuations, and its inverse $w_{t,t'}$. The correlated chi square measure for configuration i is then

$$\chi_i^2 = \sum_{t,t'} [c_i(t) - \bar{c}(t)][c_i(t') - \bar{c}(t')] w_{t,t'} \quad (4)$$

for N_t degrees of freedom. The corresponding confidence level is then used to determine the strength of deviation from the mean. For the sample of 80 configurations we treated the two time intervals $[0, N_t/2]$ and $[N_t/2 + 1, N_t - 1]$ separately. A configuration was deemed exceptional, if the confidence level determined on either interval was less than 10^{-7} , a somewhat arbitrary value that was chosen to correspond to strongly discernible deviations, many of them with the “W” shape, characteristic of an exceptional configuration. Note that a Gaussian normal fluctuation at this level in a sample of 80 would be expected only once in about 10^5 trials. The process of identifying outliers was carried out iteratively, in each pass removing the outliers from the sample as they were identified, until none remained. Results are summarized in Tables VI and VII. Based on this measure, if we were to insist on no more than one exceptional configuration in a sample of this size at $\beta = 5.7$, the NPCA would be restricted approximately to $m_\pi/m_\rho > 0.8$ and the TFCA to $m_\pi/m_\rho > 0.6$.

C. Spectrum

Correlators for the zero momentum pion, rho, nucleon, and Δ were fit to single exponential forms, minimizing the correlated χ^2 . Care is needed to prevent biases arising from the choice of the fitting range, particularly from the choice of minimum time t_{\min} . We used two methods to test for bias: In fitting correlators for a set of closely spaced κ values we selected (1) the smallest t_{\min} giving a minimum CL for all κ 's greater than 0.05 and an average CL greater than 0.1; and (2) the t_{\min} for which the product of CL and the number of degrees of freedom (df) is maximum, a rather ad hoc rule of thumb [20]. As a rule both methods gave the same t_{\min} . Where a different value was obtained, we determined that the variation in mass value was within the statistical errors of the fits.

We found that t_{\min} for the $8^3 \times 24$ lattice was generally half the value on the $16^3 \times 48$ lattice. In the few cases in which it was not (the rho meson for OFCA and TFCA), we verified that, had we enforced this further condition, the central mass value would have shifted by less than 1%, an amount smaller than the error in the observed scaling violation. Our fitting range is then approximately constant in physical units, and our results are therefore free of bias from this source.

We also checked the single exponential fits against two-exponential fits and verified that the results were stable within statistical errors. Results of the fits are shown in Table VIII.

We consider two alternatives for fixing the quark mass: (1) fixing $m_\pi^2/\sigma = 2.5$ and (2) fixing $m_\pi/m_\rho = 0.7$. These values were chosen to correspond to each other, approximately. Since variations in the strength of the clover term changes the $N - \Delta$ and $\pi - \rho$ mass splittings, so can change the pi to rho mass ratio at fixed physical quark mass, the former method is preferable. We present the second, more popular, method to allow comparison with other work.

Table IX and Figs. 4 and 5 show the masses of particles and their ratios at $m_\pi^2 = 2.5\sigma$ and the scaling violations from $6/g^2 = 5.7$ to $6/g^2 = 6.0$. For comparison, conventional Wilson data (WA) from recent calculations are shown. The WA $6/g^2 = 5.7$ values are interpolated from raw data given in Ref. [21]. The WA $6/g^2 = 6.0$ values are interpolated from raw data given in Refs. [22,23]. The value $m_\pi^2 = 2.5\sigma$ is slightly outside the range of values given in Ref. [22], so to avoid extrapolation, those data were supplemented by data given in Ref. [23]; however, extrapolation from the data

of Ref. [22] alone gives the same results. The $6/g^2 = 5.7$ NPCA values were interpolated from unpublished values provided by Heller [24]. The $6/g^2 = 6.0$ NPCA values are from Ref. [2].

The mass of the rho meson is seen to be a sensitive indicator of scaling violations. The scaling violation in the rho mass is reduced from approximately 7% for the WA to less than 2% for the OFCA and TFCA. Fattening the WA does not improve scaling with any significance. Thus smoothing of the gauge fields alone does not improve scaling. This is because the Wilson action, with either thin or fat links, has $O(a)$ lattice artifacts which are removed by the addition of the clover term. (A similar behavior for a fat link action without a clover term, in that case, a hypercubic action, was also seen in Ref. [25].)

Scaling violations of the nucleon mass are statistically consistent for all the actions considered. Scaling violations of the delta mass are improved from roughly 8% for the FWA to less than 4% for the TFCA and OFCA. This also is found for the alternative fits of the delta masses, suggesting that the scaling improvement seen is real, despite potentially large systematic errors in the fits of the delta masses.

We extrapolated the mass values to zero lattice spacing, forcing a common extrapolated mass for all actions. Our extrapolation is linear in a for the WA and FWA and linear in a^2 for the OFCA, TFCA and NPCA. Results are plotted in Figs. 4 and 5. It is clear that none of the actions completely remove scaling violations in the nucleon or delta mass, but that all of the clover actions show smaller violations than the Wilson actions.

For the second approach we adjust quark masses so as to fix the ratio $m_\pi/m_\rho = 0.7$. Table X shows the masses of particles and their ratios, and the scaling violations from $6/g^2 = 5.7$ to $6/g^2 = 6.0$. For comparison, conventional Wilson data from recent calculations are shown. The Wilson $6/g^2 = 5.7$ values are interpolated from raw data given in Ref. [21]. The Wilson $6/g^2 = 6.0$ values are interpolated from raw data given in Ref. [22]. Also shown are data for the TFCA and NPCA. For the NPCA the $6/g^2 = 5.7$ values are given in Ref. [3], already interpolated to $m_\pi/m_\rho = 0.7$. The values at $6/g^2 = 6.0$ are from Ref. [2].

The mass of the rho again is seen to be a sensitive indicator of scaling violations. For the pair of lattice spacings used, the scaling violation of the rho mass is reduced from approximately 13% for the conventional WA to less than 2% for the OFCA or the TFCA. There is no significant scaling improvement of the rho mass for the FWA compared with the WA. The scaling violations of the rho are compounded with those required by the fixing of the pion to rho mass ratio to the same constant for all cases. The quark masses are forced to values at $6/g^2 = 5.7$ and $6/g^2 = 6.0$ such that the scaling violation of the pion mass equals that of the rho mass. This roughly doubles the total rho scaling violation at fixed m_π/m_ρ , compared with that for fixed m_π , for cases where scaling violations in the pi-rho mass splittings are large, as will be shown to be the case for the Wilson actions.

Scaling violations of the nucleon mass also are compounded with those required by the fixing of the pion to rho mass ratio to the same constant for all cases. The value of the nucleon mass is lowered similarly to the pion mass by the clover (magnetic moment) term, so forcing the scaling violation of the pion mass to equal that of the rho mass also forces the nucleon mass to acquire a similar scaling violation. At $m_\pi/m_\rho = 0.7$, scaling violations of the nucleon mass are reduced from approximately 10% for the WA and FWA to approximately 5% for the TFCA to approximately 2% or lower for the OFCA.

Scaling violations of the delta mass are improved from roughly 14% for the FWA to less than 5% for the OFCA.

Mass splittings are given in Table XI at $m_\pi^2 = 2.5\sigma$. Phenomenological values of the differences of the squared masses of vector and pseudoscalar particles are almost equal for different quark flavors, so the unrealistically high quark mass used in the lattice calculations should not matter much. Similarly, the difference of the masses of spin $\frac{1}{2}$ and spin $\frac{3}{2}$ baryons are comparable for different flavors. Scaling violations of the mass splittings are reduced substantially for the clover actions compared with the Wilson actions. Also there is rough agreement with experimental values for the clover actions. The experimental values are $(m_\rho^2 - m_\pi^2) = 5.7 \times 10^5 \text{ MeV}^2$ and $m_\Delta - m_N = 294 \text{ MeV}$. Using $\sqrt{\sigma} = 468 \text{ MeV}$, we have $(m_\rho^2 - m_\pi^2)/\sigma = 2.6$ and $(m_N - m_\Delta)/\sqrt{\sigma} = 0.63$.

In summary, the proposed fat clover actions with either tree-level clover coefficient (TFCA) or optimized clover coefficient (OFCA), have greatly improved scaling properties compared with the Wilson action. The scaling improvement with either of these actions is comparable to that of the NPCA. Scaling tests of the FWA show that smoothing by itself does not improve scaling. The combination of the clover term with a fat link allows one to reach smaller values of the pseudoscalar mass than is possible with the NPCA, with an apparently equivalent level of scaling violations.

IV. CONCLUSIONS

Using a common set of gauge configurations, we have carried out a systematic study of the distribution of leading near-zero eigenvalues and the scaling of the light hadron spectrum and for a variety of fermion actions on quenched lattices with lattice spacing in the range [0.09, 0.16] fm. Actions included in this study are the conventional Wilson action (WA), Wilson action on fat gauge links (FWA), clover action with a non-perturbatively tuned clover coefficient

(NPCA), tree-level “fat” clover action (TFCA) and optimized fat clover action (OFCA). All of the clover actions show better scaling behavior than any of the Wilson actions—an entirely expected result, since adding the clover term with the correct coefficient converts an $O(a)$ action into an $O(a^2)$ one. Based on an analysis of pole positions, we have found that the fat clover actions OFCA and TFCA exhibit chiral properties superior to the NPCA, WA, and FWA. A further analysis of fluctuations in the pion correlator shows that the TFCA is far less noisy than the NPCA, a further circumstantial indication of a suppression of exceptional configurations.

ACKNOWLEDGMENTS

We thank Urs Heller for providing us with unpublished results for the nonperturbative clover action and for a careful reading of the manuscript. This work is supported in part by the U.S. National Science Foundation under grants PHY 96–01227 and PHY 99–70701 and by the U. S. Department of Energy under contract DE-FG03-95ER40894. Computations were carried out with grants of computer time for the T3E at the San Diego Supercomputer Center and for the IBM SP at the University of Utah Center for High Performance Computing.

- [1] M. Lüscher, S. Sint, R. Sommer, and P. Weisz, Nucl. Phys. **B478**, 365 (1996).
- [2] M. Gockeler et al., Phys. Rev. D **57**, 5562 (1998).
- [3] R.G. Edwards, U.M. Heller, and T.R. Klassen, Phys. Rev. Lett. **80**, 3448 (1998).
- [4] W. Bardeen, A. Duncan, E. Eichten, G. Hockney and H. Thacker, Phys. Rev. **D57**, 1633 (1998)
- [5] R. Narayanan and H. Neuberger, Nucl. Phys. **B 443**, 305 (1995).
- [6] D.B. Kaplan, Phys. Lett. B **288**, 342 (1992); Nucl. Phys. B **30** (Proc. Suppl.), 597 (1993); R. Narayanan and H. Neuberger, Phys. Lett. B **302**, 62 (1993); Phys. Rev. Lett. **71**, 3251 (1993); Nucl. Phys. B **412**, 574 (1994); Y. Shamir, Nucl. Phys. B **406**, 90 (1993); V. Furman, and Y. Shamir, Nucl. Phys. B **439**, 54 (1995).
- [7] T. DeGrand, A. Hasenfratz, and T. Kovács, Nucl. Phys. **B547**, 259 (1999).
- [8] M. Falcioni, M. Paciello, G. Parisi, B. Taglienti, Nucl. Phys. B **251** [FS13], 624 (1985); M. Albanese *et al.*, Phys. Lett. B **192**, 163 (1987).
- [9] T. DeGrand, Phys. Rev. **D60**, 094501 (1999).
- [10] T. DeGrand, A. Hasenfratz, and T. Kovács, Nucl. Phys. **B520**, 301 (1998).
- [11] A. Hasenfratz, and C. Nieter Phys. Lett. **B439**, 366 (1998).
- [12] C. Bernard and T. DeGrand, hep-lat/9909083. (To appear in the Proceedings of Lattice 99).
- [13] G. P. LePage and P. Mackenzie, Phys. Rev. **D48**, 2250 (1993).
- [14] W. Bardeen, A. Duncan, E. Eichten, G. Hockney, and H. Thacker, Nucl. Phys. (Proc. Suppl.) **B63**, 141 (1998).
- [15] Y. Kuramashi, M. Fukugita, H. Mino, M. Okawa, and A. Ukawa, Phys. Rev. Lett. **72**, 3448 (1994).
- [16] W. Bardeen, A. Duncan, E. Eichten and H. Thacker, Phys. Rev. **D59**, 014507 (1999).
- [17] Mark Stephenson, PhD Thesis (University of Utah, 1999).
- [18] R.G. Edwards, U.M. Heller, and T.R. Klassen, Nucl. Phys. **B517**, 377 (1998).
- [19] G. Bali, K. Schilling, and A. Wachter, Phys. Rev. D **56**, 2566 (1997).
- [20] K. Bitar *et al.*, Phys. Rev. D **42**, 3794 (1990).
- [21] M. Fukugita, Y. Kuramashi, M. Okawa, and A. Ukawa, Phys. Rev. Lett. **75**, 2092 (1995).
- [22] S. Aoki *et al.*, Nucl. Phys. (Proc. Suppl.) **B47**, 354 (1996).
- [23] Y. Iwasaki *et al.*, Phys. Rev. D **53**, 6443 (1996).
- [24] U.M. Heller, private communication (1998).
- [25] T. DeGrand, Phys. Rev. D **58**, 094503 (1998).

TABLE I. Guide to abbreviations for the fermion actions in this study.

FCA	Clover action on fat gauge links (either optimized or tree-level).
OFCA	Clover action on fat gauge links with optimized clover coefficient.
TFCA	Clover action on fat gauge links with tree-level clover coefficient.
NPCA	Conventional clover action with non-perturbatively tuned clover coefficient.
FWA	Wilson action on fat gauge links.
WA	Conventional Wilson action ($r = 1$).

TABLE II. Pole location $m_p a$ for small instantons

ρ/a	c_{sw}					
	1.0	1.1	1.2	1.3	1.5	1.8
1.00	-0.141	-0.073	-0.003	0.071	-	-
1.25	-0.083	-0.036	0.012	0.065	0.188	-
1.50	-0.050	-0.013	0.021	0.061	0.146	-
1.75	-0.030	-0.001	0.025	0.056	0.121	-
2.00	-0.019	0.004	0.026	0.050	0.102	0.194
2.25	-0.012	0.006	0.025	0.045	0.088	0.159
2.50	-0.009	0.007	0.023	0.041	0.078	0.138
2.75	-0.007	0.007	0.021	0.037	0.070	0.122
3.00	-0.006	0.006	0.020	0.034	0.064	0.111

 TABLE III. Pole location $m_p a$ for larger instantons

ρ/a	c_{sw}		
	1.0	1.1	1.2
2.00	-0.019	0.003	0.024
2.50	-0.008	0.005	0.020
3.00	-0.004	0.005	0.015
3.50	-0.002	0.005	0.012
4.00	-0.002	0.004	0.010
4.50	-0.002	0.003	0.009
5.00	-0.002	0.003	0.007
5.50	-0.002	0.002	0.007
6.00	-0.003	0.002	0.006

 TABLE IV. Pion masses (smeared-local channel) in lattice units vs κ for a variety of actions on quenched $12^3 \times 48$ lattices at $6/g^2 = 5.85$.

OFCA		TFCA		NPCA	
0.1200	0.621(6)	0.1220	0.539(4)	0.1300	0.733(7)
0.1210	0.547(6)	0.1230	0.463(4)	0.1310	0.645(7)
0.1220	0.465(7)	0.1240	0.378(5)	0.1320	0.547(8)
0.1230	0.370(11)	0.1245	0.319(5)	0.1330	0.432(9)
0.1235	0.316(17)	0.1250	0.260(12)	0.1335	0.364(10)

TABLE V. Continuation of table IV

FWA		WA	
0.1265	0.515(6)	0.1560	0.511(9)
0.1275	0.455(6)	0.1570	0.457(10)
0.1285	0.389(7)	0.1580	0.400(12)
0.1295	0.309(10)	0.1590	0.336(16)
0.1300	0.261(13)	0.1595	0.298(18)

TABLE VI. Outliers at $CL < 10^{-7}$ for the NPCA in a sample of 80.

κ	m_π/m_ρ	N
0.125	0.84(1)	0
0.127	0.78(1)	4
0.129	0.68(1)	5
0.1295	0.64(1)	7
0.130	0.48(2)	12
0.1302	0.50(2)	15
0.1303	0.51(3)	14

 TABLE VII. Outliers at $CL < 10^{-7}$ for the TFCA in a sample of 80.

κ	m_π/m_ρ	N
0.121	0.80(1)	0
0.122	0.75(1)	0
0.123	0.70(2)	0
0.124	0.62(2)	0
0.125	0.50(2)	2
0.126	0.42(4)	5

 TABLE VIII. Summary of hadron masses and bootstrap errors for various fat-link actions: OFCA ($c_{SW} = 1.1, 1.2$), TFCA ($c_{SW} = 1.0$), and FWA ($c_{SW} = 0.0$).

c_{SW}	$6/g^2$	κ	$m_\pi a$	$m_\rho a$	$m_N a$	$m_\Delta a$
1.1	6.0	0.1225	0.3985(21)	0.539(5)	0.807(7)	0.899(11)
1.1	6.0	0.1230	0.3549(23)	0.511(6)	0.752(8)	0.865(14)
1.1	6.0	0.1235	0.3072(25)	0.483(7)	0.691(9)	0.832(17)
1.2	5.7	0.1200	0.731(4)	0.968(7)	1.411(17)	1.58(2)
1.2	5.7	0.1220	0.569(5)	0.882(10)	1.223(24)	1.44(3)
1.0	6.0	0.1225	0.4293(20)	0.553(5)	0.841(7)	0.920(10)
1.0	6.0	0.1230	0.3891(22)	0.526(5)	0.791(7)	0.882(12)
1.0	6.0	0.1235	0.3460(25)	0.498(6)	0.737(8)	0.848(14)
1.0	5.7	0.1200	0.816(4)	0.992(5)	1.496(15)	1.630(19)
1.0	5.7	0.1220	0.682(4)	0.907(6)	1.335(16)	1.503(23)
1.0	5.7	0.1245	0.478(6)	0.802(10)	1.095(28)	1.341(29)
0.0	6.0	0.1270	0.355(3)	0.455(5)	0.725(6)	0.802(13)
0.0	6.0	0.1280	0.280(4)	0.410(5)	0.631(7)	0.743(13)
0.0	6.0	0.1290	0.186(5)	0.369(9)	0.519(13)	0.678(22)
0.0	5.7	0.1280	0.666(5)	0.780(6)	1.263(18)	1.359(17)
0.0	5.7	0.1310	0.501(7)	0.681(8)	1.073(22)	1.204(23)
0.0	5.7	0.1330	0.435(9)	0.650(8)	0.993(22)	1.151(27)

TABLE IX. Scaling summary at $m_\pi^2 = 2.5\sigma$

$6/g^2$	m_π/m_ρ	m_N/m_ρ	$m_\rho/\sqrt{\sigma}$	$m_N/\sqrt{\sigma}$	$m_\Delta/\sqrt{\sigma}$
WA					
5.7	0.815(5)	1.596(11)	1.929(21)	3.075(36)	—
6.0	0.763(2)	1.538(6)	2.072(10)	3.186(17)	—
	-6.4(0.6)%	-3.6(0.8)%	+7.4(1.3)%	+3.6(1.3)%	—
FWA					
5.7	0.823(11)	1.604(30)	1.921(26)	3.082(59)	3.362(60)
6.0	0.768(11)	1.587(21)	2.055(23)	3.261(31)	3.631(62)
	-6.6(1.7)%	-1.1(2.3)%	+7.0(1.9)%	+5.8(2.3)%	+8.0(2.7)%
TFCA					
5.7	0.704(8)	1.439(24)	2.246(29)	3.233(61)	3.733(75)
6.0	0.695(10)	1.480(23)	2.275(29)	3.366(38)	3.872(65)
	-1.3(1.8)%	+2.8(2.4)%	+1.3(1.8)%	+4.1(2.3)%	+3.7(2.7)%
OFCA					
5.7	0.678(9)	1.408(29)	2.334(34)	3.285(66)	3.814(80)
6.0	0.684(10)	1.462(24)	2.310(30)	3.384(39)	3.922(68)
	+0.9(2.0)%	+3.8(2.7)%	-1.0(1.9)%	+3.0(2.4)%	+2.8(2.8)%
NPCA					
5.7	0.671(8)	1.432(20)	2.356(30)	3.375(52)	3.854(87)
6.0	0.674(2)	1.488(9)	2.345(12)	3.490(23)	—
	+0.4(1.2)%	+3.9(1.6)%	-0.5(1.4)%	+3.4(1.7)%	—

 TABLE X. Scaling summary at $m_\pi/m_\rho = 0.7$

$6/g^2$	m_N/m_ρ	$m_\rho/\sqrt{\sigma}$	$m_N/\sqrt{\sigma}$	$m_\Delta/\sqrt{\sigma}$
WA				
5.7	1.554(16)	1.698(19)	2.638(35)	—
6.0	1.514(8)	1.924(10)	2.913(17)	—
	-2.6(1.1)%	+13.3(1.4)%	+10.4(1.6)%	—
FWA				
5.7	1.547(38)	1.710(27)	2.646(62)	3.024(71)
6.0	1.548(24)	1.905(24)	2.952(33)	3.463(61)
	+0.1(2.9)%	+11.4(2.3)%	+11.6(2.9)%	+14.5(3.4)%
TFCA				
5.7	1.436(24)	2.247(29)	3.235(61)	3.735(75)
6.0	1.475(22)	2.289(28)	3.393(37)	3.889(64)
	+2.7(2.3)%	+1.9(1.8)%	+4.9(2.3)%	+4.1(2.7)%
OFCA				
5.7	1.422(26)	2.383(33)	3.393(64)	3.893(76)
6.0	1.475(22)	2.349(29)	3.465(38)	3.968(65)
	+3.7(2.4)%	-1.4(1.8)%	+2.1(2.2)%	+1.9(2.6)%
NPCA				
5.7	1.455(9)	2.427(10)	3.532(17)	—
6.0	1.466(18)	2.380(17)	3.488(34)	—
	+0.8(1.4)%	-1.9(1.3)%	-1.2(1.1)%	—

TABLE XI. Mass splittings at $m_\pi^2 = 2.5\sigma$

$6/g^2$	$(m_\rho^2 - m_\pi^2)/\sigma$	$(m_N - m_\Delta)/\sqrt{\sigma}$
	WA	
5.7	1.22(3)	—
6.0	1.79(2)	—
	FWA	
5.7	1.19(7)	0.28(8)
6.0	1.72(6)	0.37(7)
	TFCA	
5.7	2.54(7)	0.50(10)
6.0	2.68(6)	0.51(8)
	OFCA	
5.7	2.94(8)	0.53(10)
6.0	2.84(6)	0.54(8)
	NPCA	
5.7	3.05(6)	0.48(5)
6.0	3.00(2)	—

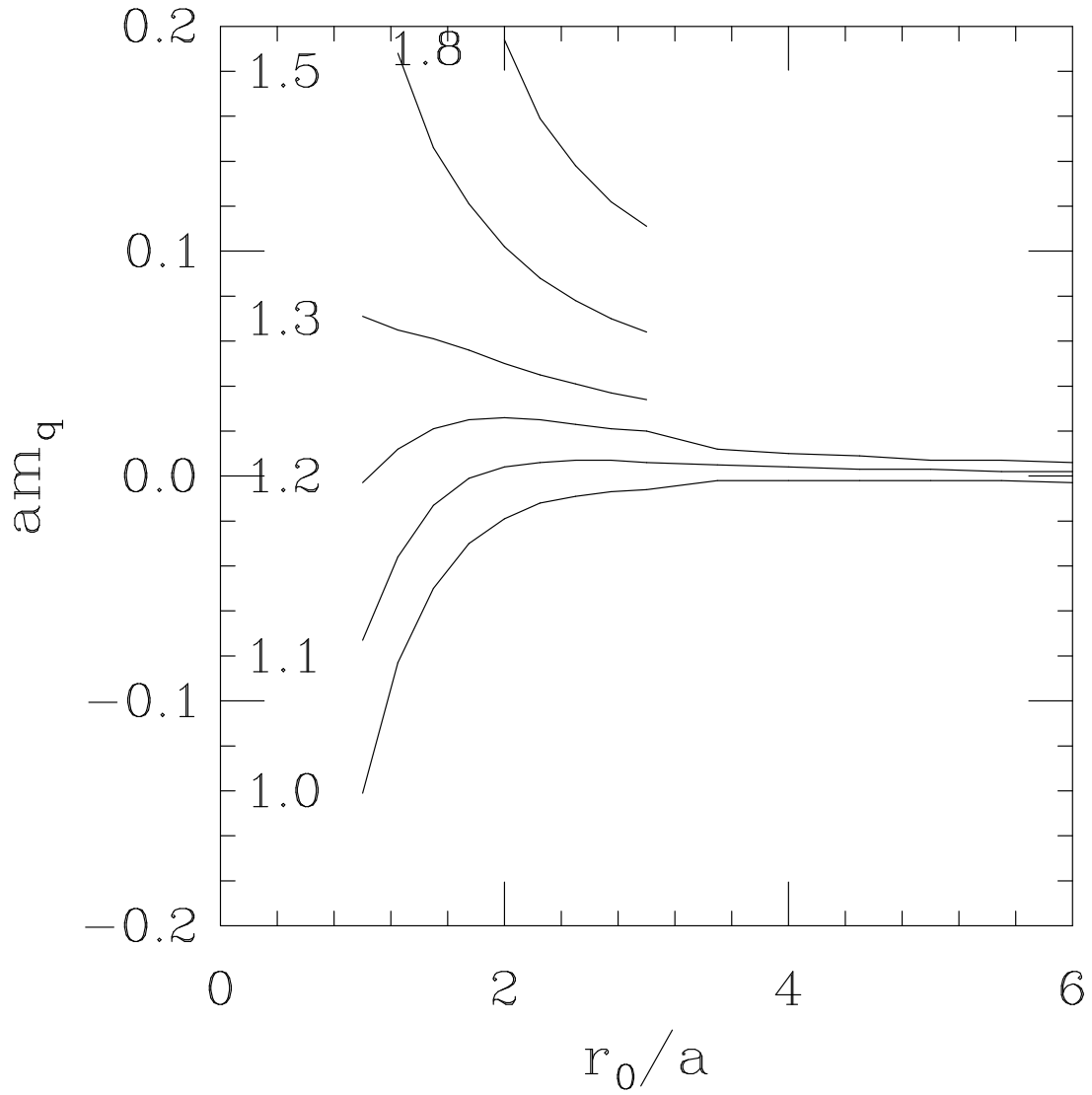


FIG. 1. Zero mode pole position expressed as a bare quark mass *vs* instanton size for artificial lattice instantons. Note that all the curves eventually approach negative infinity for small instanton sizes.

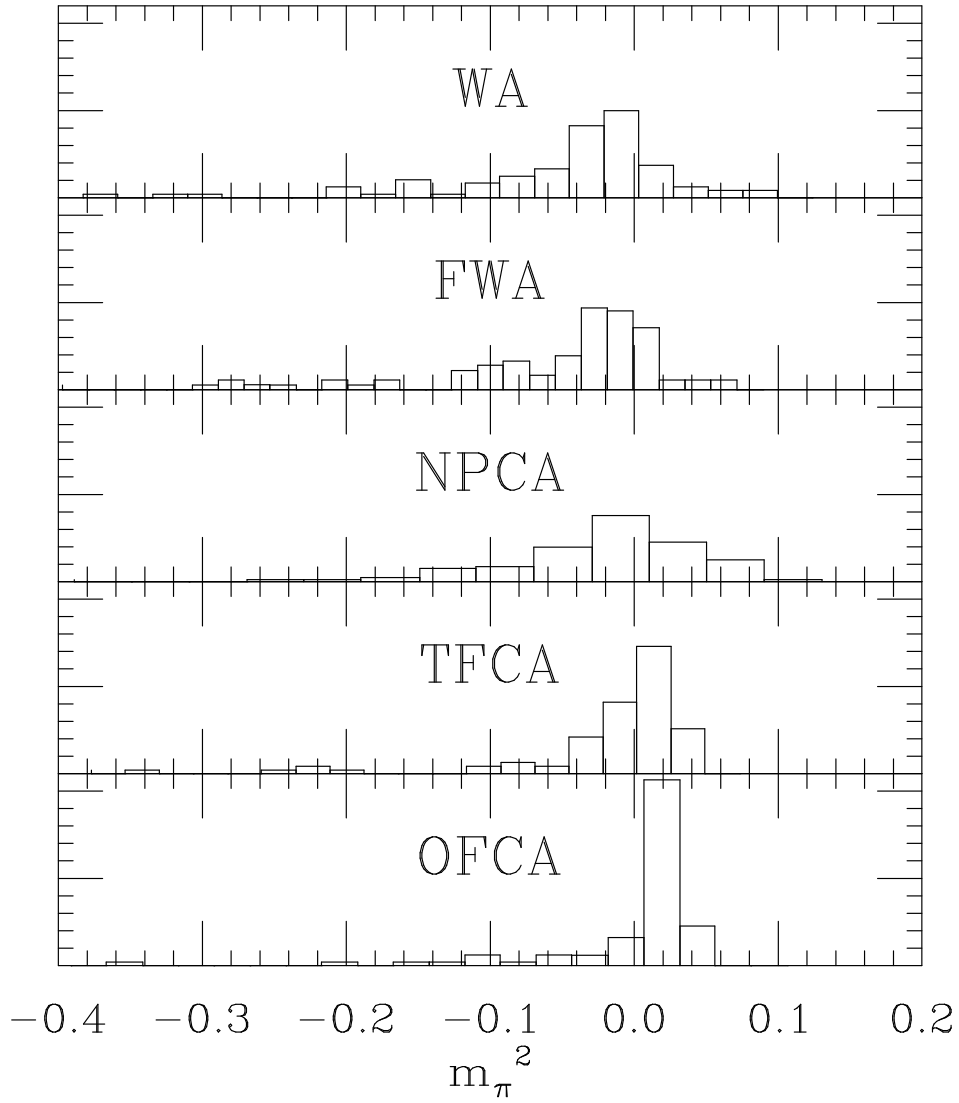


FIG. 2. Probability distribution of leading eigenvalue for various fermion actions on 100 12^4 gauge configurations at quenched $6/g^2 = 5.85$.

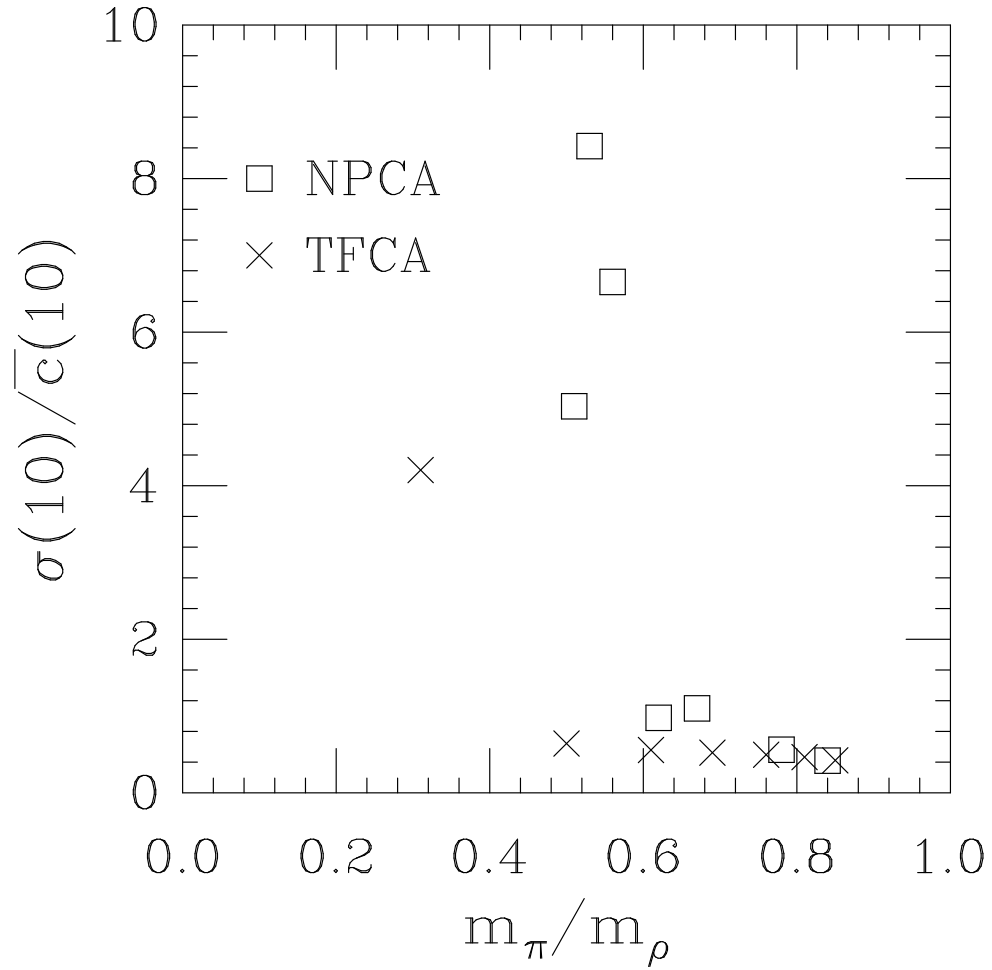


FIG. 3. Noise to signal ratio for the pion correlator at time $t = 10$ vs m_π/m_ρ for the NPCA and TFCA, on a set of 80 $8^3 \times 24$ lattices at $\beta = 5.7$.

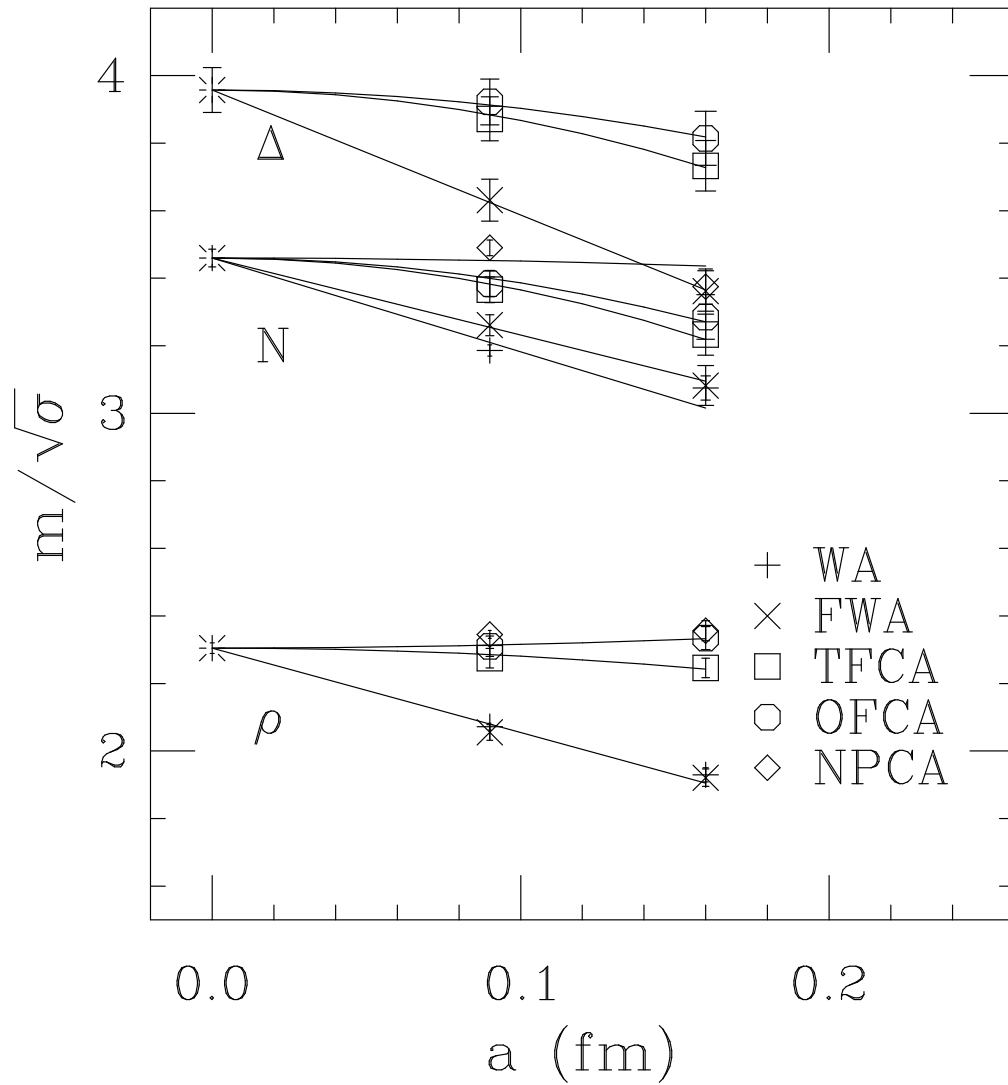


FIG. 4. Hadron masses in units of the string tension for various actions *vs* lattice spacing at fixed $m_\pi^2 = 2.5\sigma$. Masses are extrapolated to a common continuum value using a function linear in a for WA and FWA and a function linear in a^2 for the other actions.

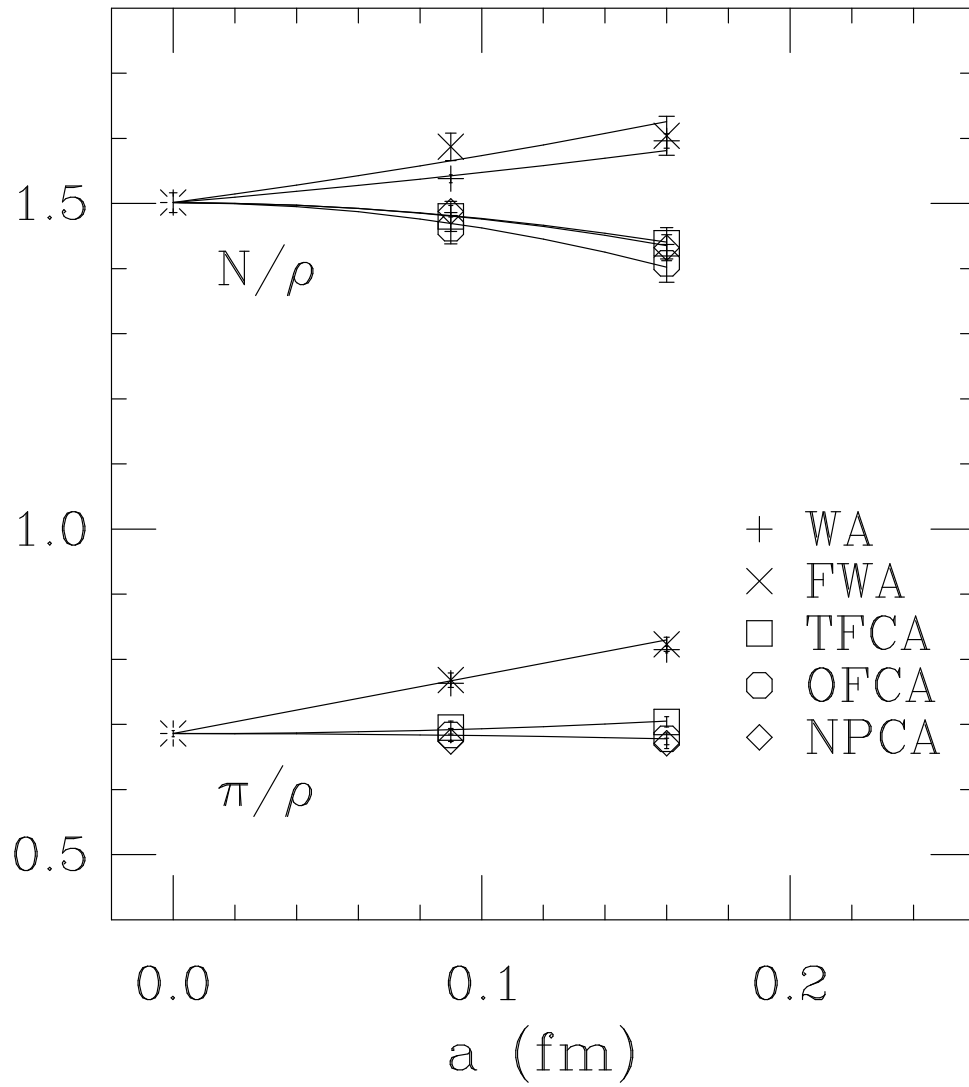


FIG. 5. Hadron mass ratios for various actions *vs* lattice spacing at fixed $m_\pi^2 = 2.5\sigma$. The extrapolation is the same as in Fig. 4.